

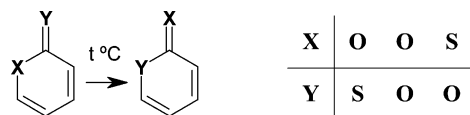
On the Pyrolysis Mechanism of 2-Pyranones and 2-Pyranthiones:
Thermally Induced Ground Electronic State Chemistry of
Pyran-2-thione

Igor Reva,* Susana Breda, Teresa Roseiro, Ermelinda Eusébio, and Rui Fausto

Department of Chemistry, University of Coimbra, 3004-535, Coimbra, Portugal

reva@qui.uc.pt

Received June 1, 2005

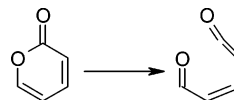


This work reports studies of thermochemistry of pyran-2-thione (PT), a sulfur derivative of α -pyrone (AP). Moderate heating of PT results in scrambling of sulfur and oxygen atoms in the molecule and formation of isomeric thiapyran-2-one (TP). The products of pyrolysis of PT were studied experimentally by a combined use low temperature matrix isolation and Fourier transform infrared spectroscopy. The infrared spectrum of the TP monomer isolated in solid argon at 10 K was completely assigned based on comparison with theoretical calculations undertaken at the DFT-(B3LYP)/6-311++G(d,p) level. The upper limit of thermal stability of PT was investigated using the differential scanning calorimetry technique. It was found that pyrolysis of PT is already initiated at temperatures below 130 °C. The mechanism of the observed pyrolytical conversion has been studied theoretically at the MP2/6-311++G(d,p) level, in the ground electronic state. The primary step of the pyrolytical reaction in PT is the α -cleavage of the C–O single bond. It proceeds via an open-ring thioketene–aldehyde structure, TK1. According to the calculations, the ring-opening reaction from PT to TK1 requires an activation energy less than 80 kJ mol⁻¹, at 130 °C, being the rate-determining step. Further steps of the pyrolytical reaction involve internal rotations around single bonds and [1,5] sigmatropic shift of the aldehydic hydrogen. Pyrolytical ring-opening reactions were studied theoretically also for AP and TP and compared to the pyrolysis of PT. It is suggested that the relative ease of the pyrolytical transformation in PT can be explained in terms of existence of the additional minimum TK1 in the reaction path. No counterparts for this structure could be theoretically located for AP and TP.

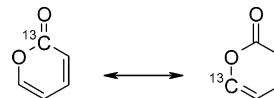
Introduction

Chemistry of 2-pyrones has been the subject of numerous studies. It has been shown that nonsubstituted α -pyrone undergoes ring opening upon UV irradiation and affords aldehyde–ketene products (Scheme 1).^{1–4} Experiments with isotopic labeling (¹³C,⁴ ¹⁸O,^{5,6} D⁷) showed migration of the label within the pyrone ring upon UV irradiation or electron impact (Schemes 2–4,

SCHEME 1



SCHEME 2



(1) Pirkle, W. H.; McKendry, L. H. *J. Am. Chem. Soc.* **1969**, *91*, 1179–1186.

(2) Pong, R. G. S.; Huang, B. S.; Laureni, J.; Krantz, A. *J. Am. Chem. Soc.* **1977**, *99*, 4153–4154.

(3) Pong, R. G. S.; Shirk, J. S. *J. Am. Chem. Soc.* **1973**, *95*, 248–249.

(4) Huang, B. S.; Pong, R. G. S.; Laureni, J.; Krantz, A. *J. Am. Chem. Soc.* **1977**, *99*, 4154–4156.

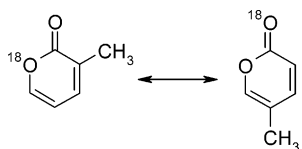
(5) Pirkle, W. H.; Turner, W. V. *J. Org. Chem.* **1975**, *40*, 1617–1620.

(6) Pirkle, W. H.; Turner, W. V. *J. Org. Chem.* **1975**, *40*, 1644–1646.

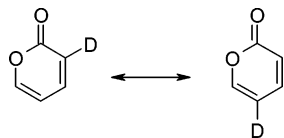
(7) Pirkle, W. H.; Dines, M. *J. Am. Chem. Soc.* **1968**, *90*, 2318–2323.

respectively). All mentioned experiments were conducted on pyrones bearing a hydrogen (or deuterium) atom in position 6. If this position was blocked by a methyl group, then the migration of the isotopic label or substituent was not observed. These experiments provided evidence that the electrocyclic ring-opening reaction in pyrone is accompanied by [1,5] sigmatropic shift of the aldehydic

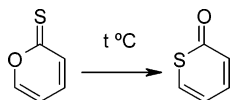
SCHEME 3



SCHEME 4



SCHEME 5



hydrogen, and that both sigmatropic shift and ring-opening reactions are reversible.

One should note that the thermochemistry of 2-pyrones is reported in the literature much less than their photochemistry. Studies of pyrolytic decarboxylation of 5-methyl-6-carboxypyrene showed apparent migration of the methyl group between the 3 and 5 positions.⁸ Concerning the studies regarding thermal rearrangements of pyran-2-thiones (PT), we are aware of only one work, which reported that, upon heating, pyran-2-thiones quantitatively afforded thiapyran-2-ones (TP) (Scheme 5).⁵ The product of pyrolysis was identified by Pirkle and Turner using NMR spectroscopy. The reaction was suggested, by analogy with photoinduced process in α -pyrone, to occur via [1,5] sigmatropic shift of the aldehydic hydrogen.

In the present study we also subjected pyran-2-thione to heating to confirm the nature of pyrolytical product(s). As could be expected, heating of pyran-2-thione resulted in formation of thiapyran-2-one, which was unequivocally identified by means of infrared spectroscopy, as will be reported later in this article. Particular emphasis in this work was given to theoretical investigation of the pyrolysis mechanisms, using high level theoretical computations. Comparison of the theoretical results obtained for pyran-2-thione, thiapyran-2-one, and α -pyrone is also given.

Results and Discussion

Matrix Isolation Data. The experimental FTIR spectrum of the products of pyrolysis of PT, deposited into an argon matrix, is presented in Figure 1 (fingerprint region) and in Figure S1 (low-frequency region). It should be noted that there are two main species identifiable in this spectrum. These are pyran-2-thione (reagent) and thiapyran-2-one (expected product). The absorptions due to the reagent, under the used conditions, are very weak, and only the strongest absorption bands could be identified.

The validity of the assignment of the PT signals is doubtless, since we have studied pyran-2-thione under

the same experimental conditions previously,⁹ and its experimental absorption spectrum is known. The species dominating in the sample can be assigned to TP. The experimental spectrum of TP (bands marked by circles) is in excellent agreement with the theoretical spectrum of the TP monomer, calculated at the B3LYP/6-311++G-(d,p) level. Internal coordinates used in the normal modes analysis of TP are given in the Supporting Information Table S1. Assignment of the experimental FTIR spectrum of TP monomer isolated in an argon matrix is given in the Supporting Information Table S2.

All calculations in this work were carried out with the Gaussian 98 program package.¹² Different methods and basis sets were used, in conformity with the problem in question. The equilibrium geometries of PT and TP were fully optimized using the B3LYP method (Becke's three parameter gradient corrected exchange functional¹³ with the gradient corrected correlation functional of Lee et al.¹⁴ and the Vosko et al.¹⁵ correlation functional) with the standard 6-311++G(d,p) basis set. Vibration frequencies calculated at the B3LYP/6-311++G(d,p) level of theory provide the best agreement with the experimental infrared spectra, compared to other theoretical methods used in this work.

The characteristic feature of the spectrum of TP is a very strong absorption band (at 1672.5 cm^{-1}) due to the stretching vibration of the C=O group. The remaining bands of TP are much weaker. However, almost all theoretically expected bands could be identified in the experimental spectrum of matrix-isolated TP after long accumulation of the spectral signal.

The experimental matrix spectrum contains a vanishingly weak band centered at 2049.6 cm^{-1} . This band can result from carbonyl sulfide (OCS).¹¹ The presence of OCS in the matrix can be explained by partial decomposition of pyran-2-thione to carbonyl sulfide and acetylene (C_2H_2) during pyrolysis. It is, however, difficult to judge whether the decomposition took place and to what extent. Both carbonyl sulfide and acetylene have low boiling points, -50 and $-28\text{ }^\circ\text{C}$, respectively. Thus, at room temperature, these products possess sufficient volatility and would easily escape from the cell during manipulations before experiment. No evidence of presence of C_2H_2 in the matrix was found, indicating that both PT and TP are chemically stable if stored at room temperature.

(9) Breda, S.; Reva, I.; Lapinski, L.; Fausto, R. *ChemPhysChem* **2005**, *6*, 602–604.

(10) Michaut, X.; Vasserot, A. M.; Abouaf-Marguin, L. *Vib. Spectrosc.* **2004**, *34*, 83–93.

(11) Lang, V. I.; Winn, J. S. *J. Chem. Phys.* **1991**, *94*, 5270–5274.

(12) Frisch, M. J.; Trucks, G. W.; Schlegel, H. B.; Scuseria, G. E.; Robb, M. A.; Cheeseman, J. R.; Zakrzewski, V. G.; Montgomery, J. A., Jr.; Stratmann, R. E.; Burant, J. C.; Dapprich, S.; Millam, J. M.; Daniels, A. D.; Kudin, K. N.; Strain, M. C.; Farkas, O.; Tomasi, J.; Barone, V.; Cossi, M.; Cammi, R.; Mennucci, B.; Pomelli, C.; Adamo, C.; Clifford, S.; Ochterski, J.; Petersson, G. A.; Ayala, P. Y.; Cui, Q.; Morokuma, K.; Malick, D. K.; Rabuck, A. D.; Raghavachari, K.; Foresman, J. B.; Cioslowski, J.; Ortiz, J. V.; Baboul, A. G.; Stefanov, B. B.; Liu, G.; Liashenko, A.; Piskorz, P.; Komaromi, I.; Gomperts, R.; Martin, R. L.; Fox, D. J.; Keith, T.; Al-Laham, M. A.; Peng, C. Y.; Nanayakkara, A.; Challacombe, M.; Gill, P. M. W.; Johnson, B.; Chen, W.; Wong, M. W.; Andres, J. L.; Gonzalez, C.; Head-Gordon, M.; Replogle, E. S.; Pople, J. A. *Gaussian 98*; Gaussian, Inc.: Pittsburgh, PA, 1998.

(13) Becke, A. D. *Phys. Rev. A* **1988**, *38*, 3098–3100.

(14) Lee, C. T.; Yang, W. T.; Parr, R. G. *Phys. Rev. B* **1988**, *37*, 785–789.

(15) Vosko, S. H.; Wilk, L.; Nusair, M. *Can. J. Phys.* **1980**, *58*, 1200–1211.

(8) Pirkle, W. H.; Seto, H.; Turner, W. V. *J. Am. Chem. Soc.* **1970**, *92*, 6984–6985.

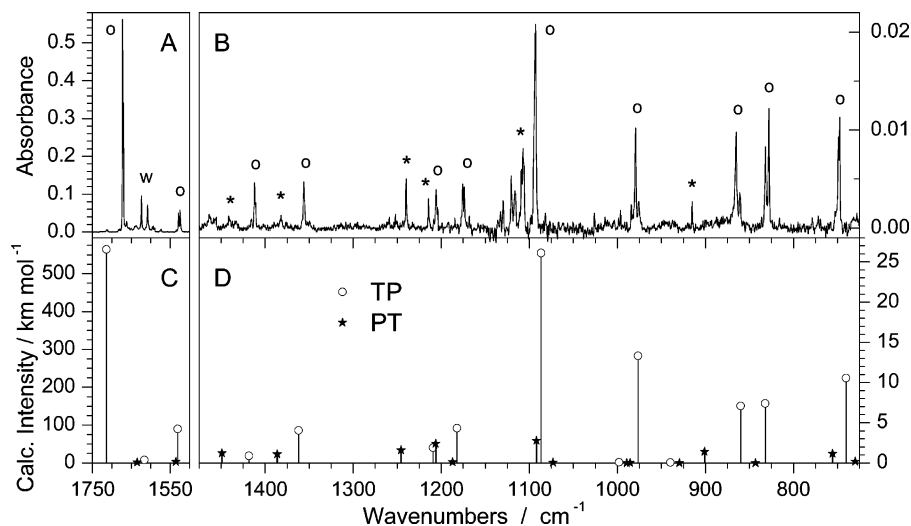


FIGURE 1. Comparison of an experimental FTIR spectrum of the product of pyrolysis of PT isolated in argon matrix at 10 K (A, B) with the theoretical spectra calculated at the DFT(B3LYP)/6-311++G(d,p) level (C, D). (○, C, D) Theoretical spectrum of TP monomer. The corresponding experimental bands due to TP (A, B) are also marked by circles. (*, C, D) Theoretical spectrum of PT monomer with intensities scaled by 0.02. Experimental bands marked by * (B) are due to the residual amount of the reagent (PT) in the matrix and are assigned on the basis of previous experiments.⁹ The pair of bands marked by “w” (A) is due to the water monomer¹⁰ present in the matrix in trace amounts. All theoretical frequencies are scaled by 0.984. Note the more than 20-fold change of the ordinate scale at 1500 cm^{-1} .

The relative amount of PT and TP in the sample was evaluated by comparing the total experimental integral intensity of the corresponding bands in the fingerprint region with the corresponding calculated intensities. This comparison gave a PT/TP ratio in the sample of ca. 1:46. It seems unrealistic to assume that saturated vapor pressures of the two species would differ so much at the experimental conditions. It is much more probable to assume that the ratio 1:46 reflects the relative amount of the two compounds in the mixture after pyrolysis. In other words, conversion of PT into TP after pyrolysis was almost 98%. The theoretical explanation of this fact will be given later in the article.

DSC Data. It was previously reported by Pirkle and Turner⁵ that pyran-2-thione rearranges completely to the isomer having sulfur in the ring. They wrote: “30% of PT converted in a single pass through a 370 °C tube. Indeed, this isomerization is so facile that it occurs extensively during attempted gas chromatography at 160 °C (150 °C injector)”.⁵ In the present work, the lowest limit of thermal stability of PT was estimated by means of differential scanning calorimetry (DSC). A sample of pyran-2-thione was subjected to a series of warming/cooling cycles. During the first warming cycle, the temperature was increased only up to 55 °C, which is only a few degrees above the melting point (Figure 2a, uppermost curve). After one minute, the sample was cooled and crystallization occurred at ca. 24 °C (Figure 2b, uppermost curve).

Subsequently, the compound was subjected to a series of consecutive heating and cooling cycles. In these scans, the upper temperature was increased and the changes in the DSC curves were monitored. All heating curves are collected in Figure 2a, and corresponding cooling curves are collected in Figure 2b, the progress of the experiment being ordered from top to bottom. All the observed transitions in the temperature range studied are presented in Figure 2a,b. Up to 100 °C, no discernible

changes were noticed either in the DSC curve profiles or in the peak onset temperature and area, indicating that up to this temperature (bold lines in Figure 2a,b, both belonging to the same cycle) pyran-2-thione does not undergo thermal conversion. Heating the sample up to 130 °C results in changes of both peak positions and line shapes as well as in the shift of the onset temperature of the main melting peak toward a lower temperature (dashed line in Figure 2a). The corresponding cooling curve (dashed line in Figure 2b) exhibits also changes in the profile, with the appearance of new peaks. A decrease in the total crystallization enthalpy is also observed. During the melting of the compound, formation of a new peak, appearing as a shoulder on the higher-temperature side of the main melting peak, can also be observed. After the first manifestation of thermal conversion, the compound was subjected to several cycles of cooling/heating with the same lower (−30 °C) and upper (+130 °C) temperature limits. The isothermal (at +130 °C) hold time of the melt was gradually increased (four lowest curves in Figure 2a,b). This resulted in further thermal conversion of the sample. The complex shapes of the corresponding melting curves as well as the broadening of the pyran-2-thione fusion peaks, together with the shift of their onset temperatures to lower values, are clear evidence of the existence of a mixture of substances.

After prolonged heating (24 h at 130 °C), the DSC cell was inflated but did not show any change in mass. After perforating the cell with a needle, a mass loss of about 15% was observed, indicating that some conversion to gaseous products had occurred. Perforation of the cell was accompanied by appearance of the characteristic smell of a sulfur-containing compound. This observation can explain the appearance of the peak due to carbonyl sulfide in the matrix spectra and evidence a possible decomposition channel of PT.

The main result of the DSC measurements is the demonstration of the fact that the thermal conversion of

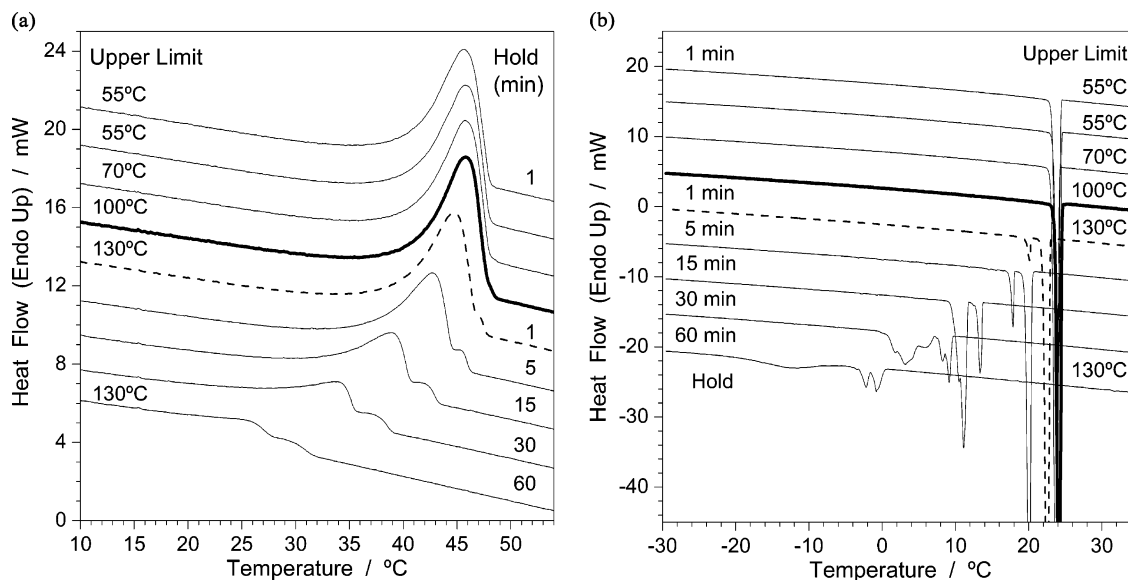


FIGURE 2. (a) Series of successive DSC melting curves of pyran-2-thione (from top to bottom). Each thermal cycle was initiated and finished at $-30\text{ }^{\circ}\text{C}$. A scan rate of $10\text{ }^{\circ}\text{C}/\text{min}$ was used. Upper temperature turning point and isothermal hold time at this temperature were varied. For each melting curve, upper conditions of the *previous* thermal cycle are indicated in the figure. For the five first cycles, molten pyran-2-thione was held for 1 min at different temperatures. For the last five cycles, the upper temperature turning point was the same and the hold time was incremented (cumulative time specified in the figure). (b) Series of successive DSC crystallization curves of pyran-2-thione (from top to bottom). Each thermal cycle was initiated and finished at $-30\text{ }^{\circ}\text{C}$. A scan rate of $10\text{ }^{\circ}\text{C}/\text{min}$ was used. Upper temperature turning point and isothermal hold time at this point were varied. For each crystallization curve, upper conditions of the *previous* melting scan are indicated in the figure. For the five first cycles, molten pyran-2-thione was held for 1 min at different temperatures. For the last five cycles, the upper temperature limit was the same and the hold time was incremented (cumulative time specified in the figure). In both a and b, the bold trace specifies the borderline condition at which no changes in the morphology of the sample and DSC curve were observed. Dashed trace specifies the lowest upper temperature limit at which transformation of pyran-2-thione started to occur.

PT starts already at moderate heating. The conversion was observed in the temperature range between 100 and $130\text{ }^{\circ}\text{C}$ (the lowest temperature for this process reported to date).

Computational Details. An important part of this study represents theoretical calculations of the pyrolysis mechanisms. As will be shown later, the reaction pathways for pyrolytical interconversions in pyran-2-thione involve bond cleavage and intramolecular proton shift in the electronic ground state. It is known that most variants of density functional theory (DFT) yield a proton transfer barrier that is considerably smaller than the best correlated conventional ab initio results, with a large polarized basis set.^{16–18} It was also reported that an accurate evaluation of ground-state intramolecular proton-transfer pathways requires the inclusion of electron correlation effects.¹⁹ One of the methods being able to provide fairly good geometry and energy parameters for the ground state is MP2.²⁰ Hence, in this study the potential energy profiles for pyrolytically relevant processes were initially calculated at the MP2/6-31G(d,p) level. In the regions of particular interest, calculations were repeated with basis sets augmented by diffuse functions, using the standard 6-31++G(d,p), 6-311+G-

(d,p), and 6-311++G(d,p) basis sets. The geometry optimizations of the stationary points at the MP2/6-311++G(d,p) level were followed by frequency calculations at the same theory level, and the obtained frequencies were used to account for the zero-point vibrational energy corrections and to confirm the nature of the stationary points found. The structures corresponding to the true local minima did not have any imaginary frequency. The transition-state geometries were identified by only one imaginary frequency. Visualization of the normal vibration, corresponding to this frequency as well as intrinsic reaction coordinate analyses,²¹ was performed on the transition structures to make sure that they led to the desired reactants and products.

To provide qualitative comparison of energies describing excited electronic states of the precursor (PT), several procedures were employed. First, for the geometry corresponding to the closed-ring PT structure, optimized at the RB3LYP/6-311++G(d,p) level, calculations of the Franck–Condon vertical excitation energies were performed using the single-excitation CI method.²² The energies of the lowest 12 excited states were calculated, and it was found that the two lowest excited states of PT are triplets, with excited singlet states being much higher in energy. The energy of the lowest triplet state was equal to 1.9759 eV (191 kJ mol^{-1}). As the next step, the closed-ring PT structure was fully optimized at the

(16) Latajka, Z.; Bouteiller, Y.; Scheiner, S. *Chem. Phys. Lett.* **1995**, *234*, 159–164.

(17) Nguyen, M. T.; Creve, S.; Vanquickenborne, L. G. *J. Phys. Chem.* **1996**, *100*, 18422–18425.

(18) Somnitz, H.; Zellner, R. *Phys. Chem. Chem. Phys.* **2000**, *2*, 1899–1905.

(19) Scheiner, S. *Acc. Chem. Res.* **1985**, *18*, 174–180.

(20) Barone, V.; Adamo, C. *J. Chem. Phys.* **1996**, *105*, 11007–11019.

(21) Gonzalez, C.; Schlegel, H. B. *J. Phys. Chem.* **1990**, *94*, 5523–5527.

(22) Foresman, J. B.; Headgordon, M.; Pople, J. A.; Frisch, M. J. *J. Phys. Chem.* **1992**, *96*, 135–149.

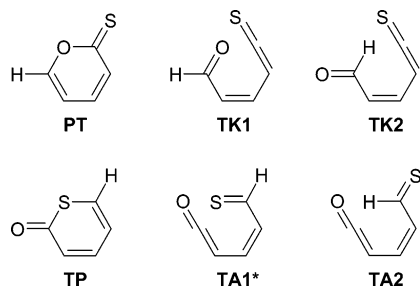


FIGURE 3. Scheme of pyrolytic conversion of PT into TP. Migrating hydrogen is shown explicitly. (*) TA1 is not a minimum.

UB3LYP/6-311++G(d,p) level as a triplet. This procedure yielded an energy difference of 211 kJ mol^{-1} (204 if account for ZPE), between the singlet ground state and the first triplet excited state (both optimized). Despite the discrepancies in the energies given by the two methods, it can be assumed that the relative energy of the lowest excited state of PT is of the order of 200 kJ mol^{-1} . On the basis of this estimation, the excited electronic states of PT will be considered in the later discussion as energetically inaccessible.

Mechanism of Pyrolysis. Previous experimental studies⁵ on pyran-2-thiones bearing a methyl substituent at the 6 position did not show any scrambling of the heteroatoms upon heating. This observation suggests that the pyrolytical transformation of the nonmethylated species includes intramolecular hydrogen atom migration and follows the mechanism depicted in Figure 3. According to this mechanism, at the primary step of the thermal conversion PT undergoes a ring-opening reaction and gives birth to the open-ring thioketene–aldehyde product (TK1). However, TK1 is not spatially prepared for the intramolecular hydrogen migration. Its rotational isomer, TK2, is the one only of eight open thioketene–aldehyde isomers⁹ suitable for this process. Upon intramolecular hydrogen transfer, a new species, open-ring thioaldehyde–ketene, is formed. It is named TA2 by analogy with its precursor, TK2. After intramolecular rotation of the thioaldehyde group, the open-ring molecule adopts the geometry TA1, suitable for the subsequent ring closure, and then TP is formed. In the forthcoming section, it will be shown why the described pyrolytical transformation from PT to TP easily occurs already at moderate heating and undergoes almost complete conversion.

Ring-Opening Reaction. The energetics of all steps of the transformation depicted in Figure 3 was studied pairwise using theoretical calculations. The first step of the reaction represents the cleavage of the O–C bond in PT. The possibility of existence of a local minimum corresponding to the open form TK1 (see Figure 3) is very important for this study. As was noted in the computational section, the best description of energy and geometry parameters is achieved at the MP2 level of theory. That is why the energy profiles for the ring-open reaction in pyran-2-thione were calculated using the MP2 method. The results are presented in Figure 4.

Initially, all calculations were performed on the planar system. A very characteristic peculiarity of the potential energy curves is the existence of a very flat region around $2.3\text{--}2.5 \text{ \AA}$, where the calculated gradients along the

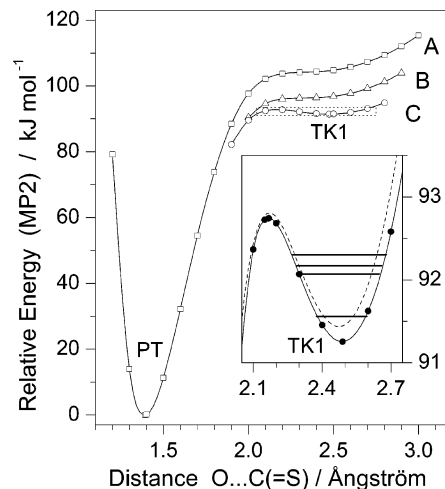


FIGURE 4. Potential energy curves for the O–C bond cleavage in PT. All calculations were carried out at the MP2 level of theory with the 6-31G(d,p) (trace A); 6-31++G(d,p) (trace B), and 6-311++G(d,p) (trace C) basis sets. For the scans presented in the mainframe, the C_s symmetry was imposed onto molecule during calculation. (Inset) Amplified view of the area designated by the dotted rectangle. The dashed line in the inset corresponds to the trace C of the mainframe (the energy scan with the planar restriction). The solid line in the inset corresponds to the calculation where the O–C distance was incrementally changed, and all other parameters, including dihedral angles, were fully optimized at the MP2/6-311++G(d,p) level. Frequency calculations were carried out at the same level of theory for the fully optimized nonplanar open-ring TK1. Energies of four lowest vibrational states of TK1 are shown in the inset as horizontal lines. The zero energy level in all cases corresponds to the energy of the closed-ring PT structure optimized at the respective level of theory.

reaction coordinate approach zero. Inflection on the potential energy surface in this region should correspond to the open-ring thioketene–aldehyde structure TK1. The region between 2.1 and 2.7 \AA was studied more carefully, without imposing any restrictions on the geometry of the system (except fixing the OC distance corresponding to the reaction coordinate). The inset in Figure 4 shows that, according to computation at the MP2/6-311++G(d,p) level, a shallow local minimum exists around 2.5 \AA . The fully optimized structure corresponding to this minimum is slightly nonplanar (the main nonplanar parameter, the $C=C-C(=S)$ dihedral angle, is less than 10°). The energy barrier separating this minimum from the closed-ring PT form is equal to 1.5 kJ mol^{-1} . A calculation carried out on the planar system is also shown for comparison (dashed line in the inset of Figure 4). As seen from the figure, assumption of planarity gives qualitatively the same result for the chosen reaction (ring-opening). The vibrational analysis performed on the optimized nonplanar structure did not reveal any imaginary frequencies. The vibrational levels corresponding to $\nu_0 \rightarrow \nu_1$ single excitations of the four lowest energy vibrational fundamentals of TK1 are situated below the barrier, which from the practical viewpoint means that the open-ring form TK1 might exist. The vibration with the lowest frequency corresponds to the torsion of the $C=C-C(=S)$ dihedral angle and connects two mirrorlike minima TK1 and TK1'. The first vibrational level of the nonplanar molecule is higher in energy than the planar

TABLE 1. Thermochemical Data, Theoretically Calculated at the MP2/6-311++G(d,p) Level of Theory, for the Species Relevant to Pyrolysis of Pyran-2-thione^a

	PT	TS1	TK1	TS2	TK2	TS3	TA2	TS4	TP
E_{el}	-665.097476	92.74	91.25	123.77	96.01	155.46	75.17	108.54	-63.20
$E_{el} + ZPE$	-665.021067		84.14		89.43		69.63		-65.23
$E_{el} + (ZPE - 1f.)$	-665.021161	85.69	84.08	114.30	89.33	137.59	69.53	99.62	-65.32
Thermochemistry (298.15 K)									
$E_{el} + E_t$	-665.014856		87.06		92.17		72.31		-65.16
$E_{el} + (E_t - 1f.)$	-665.015810	88.59	87.06	118.28	92.16	141.00	72.31	103.48	-65.17
$E_{el} + H_t$	-665.013912		87.06		92.17		72.31		-65.16
$E_{el} + (H_t - 1f.)$	-665.014866	88.59	87.06	118.28	92.16	141.00	72.31	103.48	-65.17
$E_{el} + G_t$	-665.052240		80.35		85.31		65.46		-64.40
$E_{el} + (G_t - 1f.)$	-665.050721	81.14	79.84	106.57	84.52	131.99	64.64	92.20	-65.15
Thermochemistry (400 K)									
$E_{el} + E_t$	-665.010755		87.84		92.91		73.09		-64.91
$E_{el} + (E_t - 1f.)$	-665.012031	89.32	87.83	119.26	92.91	142.11	73.08	104.56	-64.91
$E_{el} + H_t$	-665.009489		87.84		92.92		73.09		-64.90
$E_{el} + (H_t - 1f.)$	-665.010764	89.32	87.83	119.26	92.91	142.11	73.08	104.56	-64.91
$E_{el} + G_t$	-665.065987		77.94		82.85		63.00		-64.18
$E_{el} + (G_t - 1f.)$	-665.063573	78.47	77.25	102.40	81.78	128.74	61.89	88.17	-65.19

^a E_{el} : electronic energies; ($E_{el} + ZPE$): sum of electronic and the zero-point vibrational energies; ($E_{el} + E_t$): sum of electronic and thermal Energies; ($E_{el} + H_t$): sum of electronic and thermal enthalpies; ($E_{el} + G_t$): sum of electronic and thermal Gibbs free energies. Data for the reagent (PT) are given in hartrees and assumed as the zero level. Data for all other species are given in kJ mol^{-1} with respect to PT (two decimal cases are kept to show small differences). To compare thermodynamic quantities of the true minima (PT, TK1, TK2, TA2, TP) with those due to the first-order saddle points (TS1, TS2, TS3, TS4), the thermochemical data for all stationary points were additionally calculated with one lowest vibrational frequency ignored (designated as (ZPE - 1f.), ($E_t - 1f.$), ($H_t - 1f.$), ($G_t - 1f.$)). Calculations were performed for the most abundant natural isotopes and pressure equal to 1 atm. Calculations were carried out as described in the Gaussian white paper Ochterski, J. W. Thermochemistry in Gaussian (http://www.Gaussian.com/g_whitepap/thermo.htm).

structure separating two mirror TK1 minima (the minimum on the dashed line in the inset). This fact suggests that the most probable geometry for the TK1 form is effectively planar.

It is also worth commenting on the results obtained with different basis sets. It can be seen that increasing the number of the polarization and diffuse functions used in calculations results in lowering the relative energy of the plateau corresponding to the TK1 form (compare traces A, B, C in Figure 4). Usage of the split valence triple- ζ singly polarized 6-311++G(d,p) basis set (trace C) gives lower relative energies than those obtained with the split valence double- ζ basis sets (traces A, B). Finally, adding a set of f -functions to the basis results in further decrease of the relative energy in the TK1 region. The partial optimization of the open-ring structure, with the O-C distance fixed at 2.5 Å, resulted in its stabilization by more than 4 kJ mol^{-1} at the MP2/6-311++G(2df,2p) level of theory, compared to the analogous calculation at the MP2/6-311++G(d,p) level. The decrease of the relative energy in the TK1 region with the increase in the number of basis set functions favors the existence of the TK1 form and its involvement in the ring-opening thermal reaction. A remark should be made that the existence of a local minimum corresponding to the opening form TK1 was not reproduced in calculations at every theory level used in present study. This fact is in consonance with the theoretical finding reported by Latajka et al.¹⁶ They wrote: "...All types of calculation, DFT or otherwise, have surprisingly similar patterns of dependence upon basis set. The two triple- ζ singly polarized 6-311+G(d,p) and 6-311++G(d,p) sets both yield the highest barriers, which are slightly reduced when more polarization functions are added, as in 6-311++G(2df,2pd) and 6-311+G(3df,3pd)."¹⁶ Now it is clear that the potential energy profiles calculated with the double- ζ basis sets (traces A, B in Figure 4) could be

expected to produce a lower barrier. They just failed to produce a minimum in the TK1 region, since this minimum is very shallow as follows from the MP2/6-311+G(d,p) and MP2/6-311++G(d,p) calculations.

Activation Energies. Interconversion between other structures was investigated theoretically as well. There are two types of transformations: intramolecular rotations around single bonds and bond fission (or formation). Unlike the barrier separating TK1 from PT, other barriers were found to be of the order of 30–50 kJ mol^{-1} . Geometries of transition states were optimized using the synchronous transit-guided quasi-Newton (STQN) method with the quadratic synchronous transit (QST) approach.²³ For the internal rotations, the transition states were located with the QST3 option, while for bond fission (or bond formation) the QST2 option was implemented. After optimization, frequency calculations were performed on every stationary point found. The energy parameters and other relevant thermodynamic quantities were calculated at the MP2/6-311++G(d,p) level and are summarized in Table 1 for all stationary points. As can be seen from the table, account for the zero-point vibrational energies results in additional stabilization of all open-ring structures (TK, TA, and TS) with respect to the closed-ring forms (PT and TP). A possible explanation of this fact is that the reaction is not isodesmic. The closed-ring forms (PT and TP) have four single bonds and three double bonds, while the open-ring forms (TK and TA) have two single bonds and four double bonds (excluding four C-H bonds present in each case). Simple comparison shows that the ring-opening reaction produces one extra double bond at the expense of two single bonds. And the difference in the zero-point vibrational energies (which are bigger in closed forms) reflects this fact. Further

(23) Peng, C. Y.; Ayala, P. Y.; Schlegel, H. B.; Frisch, M. J. *J. Comput. Chem.* **1996**, *17*, 49–56.

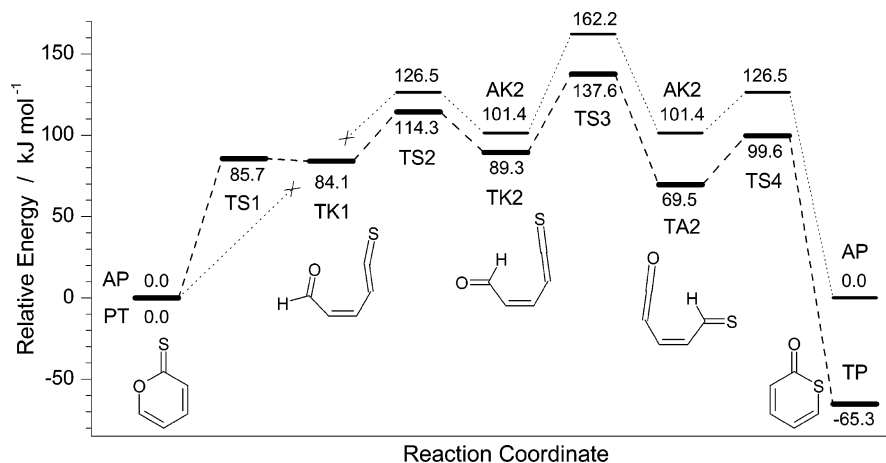


FIGURE 5. Scheme of pyrolysis of PT. Designations: (TS) transition states, (TK) open-ring thioketene-aldehyde, (TA) open-ring thioaldehyde–ketene, (TP) thiapyran-2-one, (AK) open-ring aldehyde–ketene. The zero energy level for the PT/TP family is equal to $-665.021161 E_h$. This value was calculated at the MP2/6-311++G(d,p) level of theory and corresponds to the sum of electronic and zero-point vibrational energies of PT minus one lowest vibrational frequency. The energies of all other stationary points were calculated in the same way, and their values, relative to PT, are given in kJ mol^{-1} and shown by bold traces. Thin traces show the scheme of pyrolysis of AP. AP is positioned in the figure to coincide with PT in relative energy scale. The zero energy level for the AP family is equal to $-342.451674 E_h$. All energies for the AP family were calculated using the same theory level and approach as that for the PT/TP family. Note that all transition states and minima for the AP family are symmetric in energy and structure. The minimum similar to the TK1 could not be located for open-ring aldehyde–ketene. Structures corresponding to the minima of the PT/TP family are schematically shown in the picture. The structures of the AP family (not shown) differ by the presence of the oxygen atom instead of sulfur.

analysis of Table 1 shows that, after accounting for the Gibbs free energies ($E_{el} + G_t$), all open-ring forms become even more stable, and this stabilization continues with increase in the temperature. For example, the relative energy of the TK1 form decreases from 84 kJ mol^{-1} (at 0 K) to 80 kJ mol^{-1} (at room temperature) and further to 77 kJ mol^{-1} (at 400 K, the temperature that allows the pyrolytic transformation of PT).

The numbers represented in the third row of Table 1 (i.e., the sums of electronic and zero-point energies) for the minima and transition states along the transformation path from PT to TP are presented graphically in Figure 5. The corresponding optimized geometries are summarized in Table S3 (Supporting Information). If we analyze Figure 5 for the forward reaction (from left to right), then the activation barriers for every step of transformation are equal to 85.7, 30.2, 48.3, and 30.1 kJ mol^{-1} . It is obvious that the ring-opening reaction (the initial step of the process) is the rate-determining step. As soon as the system possesses enough energy to surmount the initial barrier, the following steps should occur relatively easily and rapidly. The final product, thiapyran-2-one, is stabilized by ca. 65 kJ mol^{-1} with respect to pyran-2-thione, and the reaction as a whole is highly exergonic. The reaction in the reverse direction (from TP to PT) would face the barrier of 165 kJ mol^{-1} at the initial step. This almost 2-fold difference in the activation energies for the forward and reverse processes explains why PT was found to convert almost completely into TP, as evidenced by the matrix-isolation data (Figure 1).

The pyrolytical ring-opening reaction in α -pyrone (AP) was also simulated in this study. The energy diagram for the α -pyrone family is presented in Figure 5 along with data for the PT/TP system. The fact to be stressed here is that the activation energy for the ring-opening reaction in AP was calculated to be $126.5 \text{ kJ mol}^{-1}$, which

is much higher than that in PT. The geometry of the corresponding transition-state structure is characterized by the aldehyde group rotated by ca. 90° with respect to the plane formed by the remaining heavy atoms. The transition state for the hydrogen shift was also located. Its relative energy with respect to AP was found to be $162.2 \text{ kJ mol}^{-1}$. The geometries of the two transition states in the pyrolysis of α -pyrone are similar to those of the transition states (TS2 and TS3) on the path from PT to TP, but their energies are systematically higher.

The ring-opening reaction represents the rate-determining step for pyrolysis in all three related systems (PT, TP, and AP). Calculated potential energy profiles for this reaction in PT, TP, and AP are shown in Figure 6. Pyran-2-thione is the only one of the three systems that has a flat region on the higher-energy wing of the potential curve. No such peculiarity was found for either TP or AP. In TP, the theoretical search for a minimum with thioaldehyde and ketene groups oriented toward each other was unsuccessful. During geometry optimization, when the thioaldehyde group was oriented toward the ketene moiety, the structure was always converging to the closed-ring TP form at any level of theory. A similar result was reported by Birney,²⁴ who studied α -pyrone in terms of the ring closure (or opening, if seen from the other perspective). He wrote: “Although the flatness of the plateau on the potential energy surface depends on the level of theory, at none of the correlated levels is there a minimum in the vicinity of the [...] structure for zZz1” (by Birney, the zZz1 is the open-ring form obtained from AP, in the same way as the TK1 form was obtained from PT in this study). The calculations of the ring cleavage reaction in AP, carried out in the present work at the higher theory level, did not result in a minimum on the open-ring side either. These results mean that, to obtain

(24) Birney, D. M. *J. Org. Chem.* **1996**, *61*, 243–251.

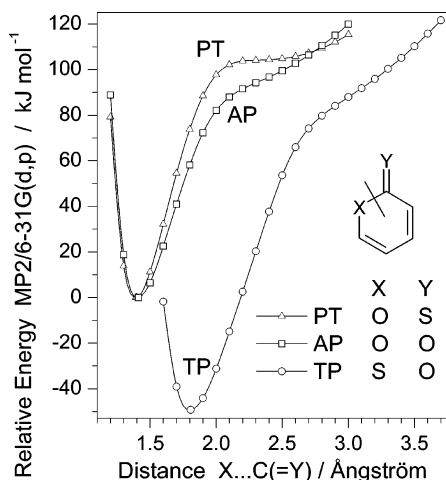


FIGURE 6. Potential energy curves for ring opening in PT, AP, and TP, calculated at the MP2/6-31G(d,p) level of theory. The bond corresponding to the reaction coordinate is crossed by a line. For simplicity, calculations were carried out with restriction of planarity. The zero level is equal to $-664.961870 E_h$ for PT and TP. The curve for AP was placed in the plot in such a way that its minimum for the closed-ring structure would coincide in ordinate with the minimum for PT. The zero level for AP is equal to $-342.383546 E_h$.

a stable open-ring structure from TP or AP, the process should involve changes of two internal coordinates (bond fission accompanied by an internal rotation). Such a situation would imply higher activation energies for pyrolytical reactions in TP and AP. In the case of TP, this result is consistent with our matrix results: even at 200 °C the pyrolytical reaction is essentially a one-way process. There is not enough energy at 200 °C to afford the reverse reaction. This is also true for AP. Pirkle et al. studied the pyrolysis of α -pyrone and wrote about it: “The requisite activation energy apparently can be acquired at $\sim 500^\circ$ and the sigmatropic shift consequently follows the pyrolytic reaction”.⁸

The only difference in the pyrolytic processes occurring in PT and AP is the existence of the TK1 minimum in the former case, which drastically reduces the activation energy of the first, rate-determining, step of the thermal reaction. Once populated, the TK1 acts as a launching pad for further transformations in PT. The existence of this additional minimum logically explains the experimentally observed ease of pyrolysis of PT. Furthermore, the highest transition states in pyrolysis of both PT and AP are associated with the intramolecular hydrogen shift. The relative energies of these transition states with respect to the closed-ring species differ by less than 18% in both systems. The experimentally observed pyrolysis temperatures are, however, quite different. This should imply that the pyrolysis process goes in a stepwise manner rather than in a concerted way. The experimental confirmation of such conclusion may be found in a series of works of Chuchani and coauthors (see, for example, refs 25 and 26), who found that pyrolytical reactions with calculated activation energies in the range $150\text{--}180 \text{ kJ mol}^{-1}$ (like in AP) usually occur at temperatures well above 300 °C. On the other hand, for

octanitrocubane, the compound with the calculated activation energy of pyrolysis equal to $86.65 \text{ kJ mol}^{-1}$ (like in PT), the experimental value of the decomposition temperature was reported to be equal to 200 °C.^{27,28}

Intramolecular Hydrogen Shift. Now let us have a closer look at the intramolecular hydrogen migration. The reaction was investigated in two directions, forward (from TK2 to TA2) and backward (from TA2 to TK2). For the forward reaction, the theoretically calculated energy profiles and related geometry parameters are presented in Figure 7a. The reaction coordinate (abscissa in the lower frame) was chosen as the distance between the migrating hydrogen atom and the carbon atom on the opposite side of the carbon chain. Variation of the reaction coordinate practically did not change the length of the existing aldehydic C–H bond for the most part of the reaction path (Figure 7a, circles in the upper frame). Instead, the curvature of the carbon chain was smoothly increasing, or in other terms, the distance between the terminal carbon atoms of the molecule was smoothly, practically linearly, decreasing (Figure 7a, squares in the upper frame). This change continued until ca. 1.3 Å, when the $\text{H}\cdots\text{C}(=\text{O})$ (Figure 7a, upper frame) and $\text{H}\cdots\text{C}(=\text{S})$ (Figure 7a, lower frame) distances became practically equal, and then the molecule abruptly transformed into its counterpart, with concomitant drastic decrease in energy and change in geometry. The results for the backward reaction are presented in Figure 7b and are very similar. The only important difference is that, upon completion of the reaction, the energy of the system increases.

The transition-state TS3 obtained in the two reactions (forward and reverse) was the same, even though the molecules approached it in a different way. However, in both cases, the molecule left the transition state in a similar abrupt manner. This observation might reflect the fact that the proper reaction coordinate for the intramolecular proton migration should not be the change of the $\text{C}\cdots\text{H}$ distance, but mainly the change in the curvature of the carbon chain. However, the real reaction coordinate probably involves the simultaneous change of many geometrical parameters and is too difficult to simulate theoretically. Nevertheless, the choice of the reaction coordinate is not that important, since the transition state obtained in the two simulations shown in Figure 7 was the same. Additionally, the same transition state (TS3) was obtained by a direct optimization using the QST2 method, using TK2 and TA2 structures as terminal points.

The optimized geometry of the transition state for the intramolecular proton shift between thioaldehyde–ketene and thioketene–aldehyde (TS3) is shown in Figure S3. At first glance, it is clear that the geometry of the carbon backbone of TS3 reminds a closed-ring structure. The optimization at the MP2/6-31G(d,p) level shows that the distance between the terminal C atoms is equal to 2.41 Å in the closed-ring PT molecule. In contrast, in the TA2 and the TK2 forms this distance is equal to 3.15 and 3.23 Å, respectively. The corresponding

(26) Chuchani, G.; Marquez, E.; Herize, A.; Domínguez, R. M.; Tosta, M.; Brusco, D. *J. Phys. Org. Chem.* **2003**, *16*, 839–848.

(27) Zhang, J.; Xiao, H. M. *J. Chem. Phys.* **2002**, *116*, 10674–10683.

(28) Eaton, P. E.; Gilardi, R. L.; Zhang, M. X. *Adv. Mater.* **2000**, *12*, 1143–1148.

(25) Chamorro, E.; Quijano, J.; Notario, R.; Sánchez, C.; León, L. A.; Chuchani, G. *Int. J. Quantum Chem.* **2003**, *91*, 618–625.

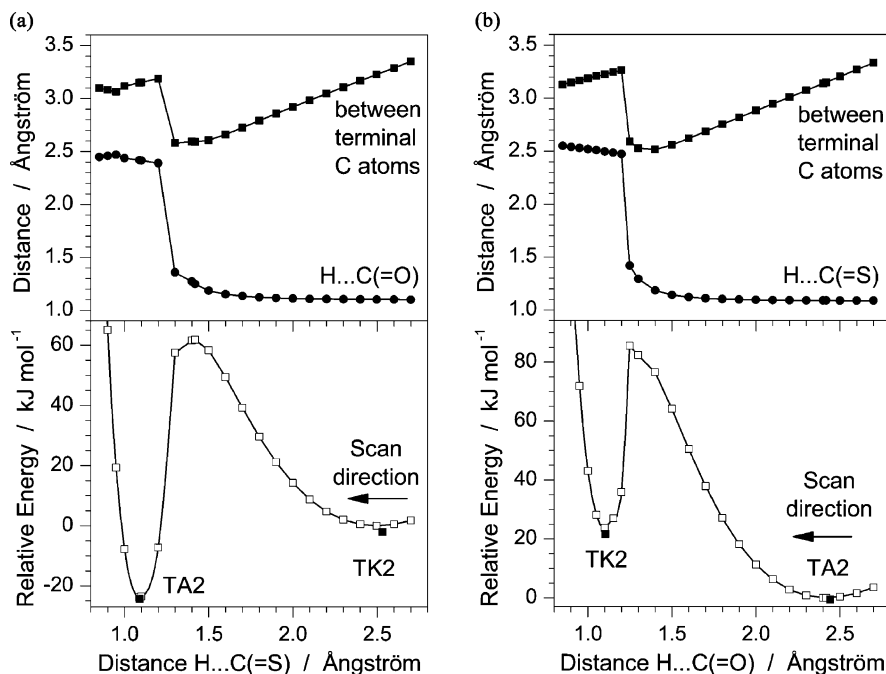


FIGURE 7. (a) Theoretical study of the intramolecular hydrogen transfer transforming open-ring TK2 into open-ring TA2. Calculation at the MP2/6-31G(d,p) level of theory with the C_s symmetry imposed on the molecule. Lower frame: potential energy curve. The zero energy level is equal to $-664.917622 E_h$ and corresponds to the energy of the starting geometry, the planar counterpart of the TK2 form. The energies of the nonplanar optimized TK2 and TA2 structures are shown by black squares for comparison. Upper frame: optimized geometric parameters. (■) Distance between the terminal carbon atoms of the open chain molecule. (●) Distance between the H atom which is being transferred and the C atom from which it is being detached. (b) Theoretical study of the intramolecular hydrogen transfer transforming open-ring TA2 into open-ring TK2. Calculation at the MP2/6-31G(d,p) level of theory with the C_s symmetry imposed on the molecule. Lower frame: potential energy curve. The zero energy level is equal to $-664.926647 E_h$ and corresponds to the energy of the starting geometry, the planar counterpart of the TA2 form. The energies of the nonplanar optimized TK2 and TA2 structures are shown by black squares for comparison. Upper frame: optimized geometric parameters. (■) Distance between the terminal carbon atoms of the open chain molecule. (●) Distance between the H atom which is being transferred and the C atom from which it is being detached.

geometric parameter for the TS3 structure is 2.58 Å, which is much closer to the closed ring.

It is also worth commenting on the symmetry of the transition state. According to Woodward and Hoffmann,^{29,30} if the observed process is a [1,5] sigmatropic hydrogen shift, the orbital symmetry relationships shall play a determinant role in the course of the transformation. The symmetry-allowed thermal [1,5] hydrogen shift should occur as a suprafacial process, and the saddle-point geometry (in the ground electronic state) should possess a plane of symmetry (and not an axis). This is exactly the case found in this study for the transition state for hydrogen migration in the conjugated aldehyde–ketene (open-ring product of α -pyrone, see Figure S4). Figure S4 shows that the migrating hydrogen atom is shifted aside from the plane of carbon atoms (rather than being on the C_2 axis) and two oxygen atoms are shifted to the opposite side. The overall structure of the transition state is C_s (and not C_2). In the similar process transforming conjugated thioaldehyde–ketene into aldehyde–thioketene, the highest possible molecular symmetry is reduced because of the substitution of one oxygen atom by sulfur. However, the geometry of the transition state in this case is very similar to that one

found for the aldehyde–ketene derivative of AP, and the hydrogen migration process can also be described as having the suprafacial character.

Conclusions

This work reports studies of the thermally induced chemistry of pyran-2-thione. The product of pyrolysis of pyran-2-thione was deposited into an argon matrix at 10 K. The product has been unequivocally characterized using infrared spectroscopy as thiapyran-2-one. Matrix isolation data show that the conversion of PT into TP was almost complete after prolonged heating at 200 °C. The limit of thermal stability of pyran-2-thione has been studied by means of DSC. It was found that the thermal conversion of PT starts at temperatures below 130 °C. The reaction pathways for the pyrolysis of PT were calculated at the MP2/6-311++G(d,p) level of theory. In addition to pyran-2-thione, pyrolysis pathways were also calculated for the two related systems, thiapyran-2-one and α -pyrone. It was shown that pyran-2-thione is the only one of the three systems that possesses an additional open-ring conformer TK1. The existence of this conformer reduces the activation energy for the ring-opening reaction in pyran-2-thione to less than 90 kJ mol⁻¹. The bond cleavage represents the rate-determining step of the pyrolytical reactions in all three systems. Further steps include intramolecular rotation along the single C–C

(29) Woodward, R. B.; Hoffmann, R. *J. Am. Chem. Soc.* **1965**, *87*, 2511–2513.

(30) Woodward, R. B.; Hoffmann, R. *Angew. Chem., Int. Ed.* **1969**, *8*, 781–853.

bonds and intramolecular [1,5] sigmatropic proton shift. These steps require smaller activation energies compared to that of the ring-opening reaction. The high directionality of the pyrolytical reaction in PT results from the fact that the final product of the reaction, thiapyran-2-one, lies much lower in energy than the reagent, and the pyrolytical reaction in the opposite direction is inhibited by a very high activation barrier.

Experimental Section

The sample of pyran-2-thione was obtained as described in ref 9. A part of the sample, intended for pyrolysis, was placed into a Pyrex glass tube protected against light. The tube with compound was purged by a flux of argon for half an hour and sealed. The sealed tube was then subjected to 2 h of heating at ca. 200 °C in an oven protected from light. After thermal treatment, the glass seal was opened and the forward end of the tube was connected to a needle valve³¹ suitable for further deposition of the matrixes. During deposition of the matrix,

(31) Reva, I. D.; Stepanian, S. G.; Adamowicz, L.; Fausto, R. *J. Phys. Chem. A* **2001**, *105*, 4773–4780.

(32) Reva, I. D.; Jarmelo, S.; Lapinski, L.; Fausto, R. *J. Phys. Chem. A* **2004**, *108*, 6982–6989.

(33) Nunes, S. C. C.; Eusébio, M. E.; Leitão, M. L. P.; Redinha, J. S. *Int. J. Pharm.* **2004**, *285*, 13–21.

(34) Sabbah, R.; An, X. W.; Chickos, J. S.; Leitão, M. L. P.; Roux, M. V.; Torres, L. A. *Thermochim. Acta* **1999**, *331*, 93–204.

the rear end of the tube containing the products of pyrolysis was kept at 0 °C. A CsI window was used as optical substrate for matrixes. Argon N60 was used as the matrix gas host. Infrared spectra were registered with a resolution of 0.5 cm⁻¹ in the range 4000–400 cm⁻¹. The Fourier transform infrared spectrometer and low-temperature equipment are described elsewhere.³²

The thermal stability of pyran-2-thione was studied by DSC using a power compensation instrument.³³ Purge was performed with a helium flux (20 mL/min). Aluminum pans (40 μL) suitable for volatile substances were used. The temperature during cooling/heating runs was scanned at 10 °C/min rate. The instrument was calibrated³⁴ for temperature with 99.99% indium and 99.9% biphenyl and for enthalpy with indium.

Acknowledgment. The financial support from the Portuguese Foundation for Science and Technology (FCT Grants No. SFRH/BPD/1661/2000, SFRH/BD/16119/2004, and POCTI/QUI/58937/2004) and FEDER is acknowledged.

Supporting Information Available: Computed Cartesian coordinates for all structures, experimental and computed vibrational spectra, band assignments, and potential energy distributions for thiapyran-2-one. This material is available free of charge via the Internet at <http://pubs.acs.org>.

JO051100W